

# Learn from Your Mistakes: Self-Correcting Masked Diffusion Models

**Yair Schiff**<sup>1\*</sup> **Omer Belhasin**<sup>2\*</sup> **Roy Uziel**<sup>2</sup> **Guanghan Wang**<sup>1</sup> **Marianne Arriola**<sup>1</sup> **Gilad Turok**<sup>1</sup>  
**Michael Elad**<sup>2†</sup> **Volodymyr Kuleshov**<sup>1†</sup>

<sup>1</sup>Cornell <sup>2</sup>NVIDIA

## Abstract

Masked diffusion models (MDMs) have emerged as a promising alternative to autoregressive models, enabling parallel token generation while achieving competitive performance. Despite these advantages, MDMs face a fundamental limitation: once tokens are unmasked, they remain fixed, leading to error accumulation and ultimately degrading sample quality. We address this by proposing a framework that trains a model to perform both unmasking and correction. By reusing outputs from the MDM denoising network as inputs for corrector training, we train a model to recover from potential mistakes. During generation we apply additional corrective refinement steps between unmasking ones in order to change decoded tokens and improve outputs. We name our training and sampling method *Progressive Self-Correction* (*ProSeCo*) for its unique ability to iteratively refine an entire sequence, including already generated tokens. We conduct extensive experimental validation across multiple conditional and unconditional tasks, demonstrating that *ProSeCo* yields better quality-efficiency trade-offs (up to  $\sim$ 2-3x faster sampling) and enables inference-time compute scaling to further increase sample quality beyond standard MDMs (up to  $\sim$ 1.3x improvement on benchmarks).

## 1. Introduction

Masked diffusion models (MDMs) have emerged as a powerful paradigm for discrete data generation, offering a compelling alternative to standard autoregressive (AR) models (Lou et al., 2024; Ou et al., 2024; Sahoo et al., 2024a; Shi et al., 2024). By treating generation as a denoising pro-

cess that gradually unmasks tokens in parallel, MDMs can achieve efficiency gains and maintain sample quality across various domains, including natural language processing and molecular design (Schiff et al., 2024), and have even demonstrated competitive performance from the 8B scale (Nie et al., 2025) up to 100B parameters (Bie et al., 2025).

However, a fundamental limitation persists for MDMs: once a token is unmasked, it remains fixed for the duration of the generation process. Consequently, errors made during parallel decoding inevitably accumulate, leading to distributional drift and degraded sample quality. While recent work has begun to explore error correction for MDMs (Lezama et al., 2023; Zhao et al., 2024b; Wang et al., 2025a; Huang et al., 2025; Kim et al., 2025a; Liu et al., 2026), efficiently identifying which tokens require modification and altering them remains a significant challenge.

In this work, we address this limitation by proposing a principled framework that equips MDMs with the inherent ability to both decode and correct. Our key insight is to treat model-generated outputs as corrupted versions of the true data, where errors represent a form of noise that can be undone through a nested corrector loop. Our method therefore trains a model to recover the clean signal from its own potentially mistaken outputs, enabling it to learn from and correct its own failure modes. We implement this training via a simple additional cross-entropy loss term added to standard MDM objectives. During inference, we leverage this capability by interleaving corrective steps in between standard unmasking steps, allowing the model to dynamically refine and “self-correct” outputs. The training and inference modifications we make to existing MDM algorithms are minimal, yet lead to marked gains. We name our approach *Progressive Self-Correction* (*ProSeCo*), since our method has the ability to iteratively refine all positions in a sequence, including ones already unmasked.

On math and coding benchmarks, our method significantly improves standard fine-tuning of large MDMs, enabling  $\sim$ 2-3x faster generation without quality degradation, and up to  $\sim$ 1.3x increase in benchmark accuracy. For guided generation, we demonstrate that recovering from mistaken tokens improves the Pareto frontier of sample quality and prop-

\*Equal contribution †Equal senior authorship . Correspondence to: Yair Schiff <yairschiff@cs.cornell.edu>, Omer Belhasin <obelhasin@nvidia.com>.

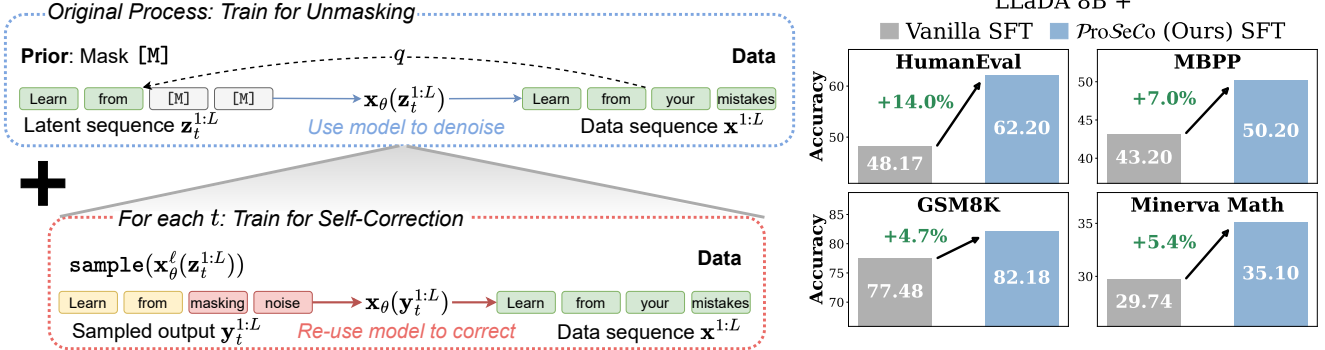


Figure 1. (Left) Overview of training *ProSeCo*: The original process trains the model to generate via unmasking. For every timestep in the masking process, we train the model to undo corruptions that can arise from sampling from the model’s unmasking predictions, thereby training for self-correction. (Right) Using our method to supervised fine-tune (SFT) the 8B parameter LLaDA model (Nie et al., 2025) significantly outperforms SFT with vanilla masked diffusion modeling.

erty maximization. Finally, we also demonstrate that for unconditional generation, our method improves over MDMs and other proposed correctors in terms of generating fluent text without collapsing the diversity of generated outputs. Across all experiments we demonstrate that *ProSeCo* better trades-off quality and speed, and can also benefit from inference-time scaling to further increase sample quality.

In summary, our contributions are as follows:

1. We present a framework that jointly trains a model to decode masked tokens and correct mistakes.
2. We provide easy-to-implement training and sampling algorithms for our model that entail only minor additions to standard MDM procedures.
3. We conduct a comprehensive experimental study demonstrating that *ProSeCo* outperforms baseline discrete diffusion models in terms of quality-efficiency trade-offs and enables inference-time compute scaling to further improve quality beyond standard MDMs.

## 2. Background

**Discrete Diffusion** Diffusion is a paradigm for generative modeling where a denoising process  $p_\theta$  is trained to undo a pre-defined corruption process  $q$  (Sohl-Dickstein et al., 2015; Song & Ermon, 2019; Song et al., 2020). Starting from data  $\mathbf{x} \sim q_{\text{data}}$ , the corruption process produces latent variables  $\mathbf{z}_t \sim q(\mathbf{z}_t \mid \mathbf{x})$  for  $t \in [0, 1]$ , which increasingly move further from the data and towards noise, as  $t$  increases.

Adapting diffusion models to discrete data requires a corruption process over the space of sequences of tokens with values in a finite vocabulary (Austin et al., 2021a). To denote this data, we let  $\mathbf{x}, \mathbf{z}_t \in \mathcal{V}$ , where  $\mathcal{V} := \{0, 1\}^V \subset \Delta^V$ , and  $\Delta^V$  denotes the probability simplex over  $V$  categories.

We use superscripts to denote the sequence dimension; for example,  $\mathbf{x}^{1:L} \in \mathcal{V}^L$  represents a sequence of tokens  $(\mathbf{x}^1, \dots, \mathbf{x}^L)$ , where token  $\mathbf{x}^\ell \in \mathcal{V}$ , for  $\ell \in \{1, \dots, L\}$ .

**Masked Diffusion Models** A promising instantiation of the discrete diffusion paradigm is the recent line of masked diffusion models (MDM; Lou et al. (2024); Ou et al. (2024); Sahoo et al. (2024a); Shi et al. (2024)). In this framework, the corruption process is characterized by marginals that interpolate between data and noise:

$$q(\mathbf{z}_t \mid \mathbf{x}) = \text{Cat}(\mathbf{z}_t; \alpha_t \mathbf{x} + (1 - \alpha_t) \mathbf{m}), \quad (1)$$

where  $\mathbf{m}$  denotes the one-hot vector for a special `[M]` token and  $\alpha_t := \alpha(t) \in [0, 1]$  is a noise schedule that is monotonically decreasing in  $t$ . In MDM, the corruption process is defined to be ‘absorbing,’ meaning that once a token transitions to the masked state, it remains in this state.

Diffusion models are trained via a variational bound on the negative log-likelihood (NLL). This bound encourages the learned approximate posterior  $p_\theta(\mathbf{z}_s \mid \mathbf{z}_t)$  to match the true one  $q(\mathbf{z}_s \mid \mathbf{x}, \mathbf{z}_t)$ , for  $s < t$  (Sohl-Dickstein et al., 2015). For MDMs, the true posteriors take the following form (Austin et al., 2021a; Sahoo et al., 2024a):  $q(\mathbf{z}_s \mid \mathbf{x}, \mathbf{z}_t) =$

$$\begin{cases} \text{Cat}(\mathbf{z}_s; \mathbf{z}_t) & \mathbf{z}_t \neq \mathbf{m}, \\ \text{Cat}\left(\mathbf{z}_s; \frac{\alpha_s - \alpha_t}{1 - \alpha_t} \mathbf{x} + \frac{1 - \alpha_s}{1 - \alpha_t} \mathbf{m}\right) & \mathbf{z}_t = \mathbf{m}. \end{cases} \quad (2)$$

A common parameterization for  $p_\theta(\mathbf{z}_s \mid \mathbf{z}_t)$  replaces  $\mathbf{x}$  in (2) with the output of a neural network:  $\mathbf{x}_\theta(\mathbf{z}_t) \in \Delta^V$ . Taking the continuous-time limit of the diffusion process, the variational objective (NELBO) for MDMs simplifies to (Ou et al., 2024; Sahoo et al., 2024b; Shi et al., 2024):

$$\mathcal{L}_{\text{NELBO}}^{\text{MDM}}(\theta) := \quad (3)$$

$$\mathbb{E}_{q_{\text{data}}} \int_0^1 \mathbb{E}_{q_t} \sum_{\ell=1}^L \delta_{\mathbf{z}_t^\ell, \mathbf{m}} \frac{\dot{\alpha}_t}{1 - \alpha_t} \log \langle \mathbf{x}_\theta^\ell(\mathbf{z}_t^{1:L}), \mathbf{x}^\ell \rangle dt,$$

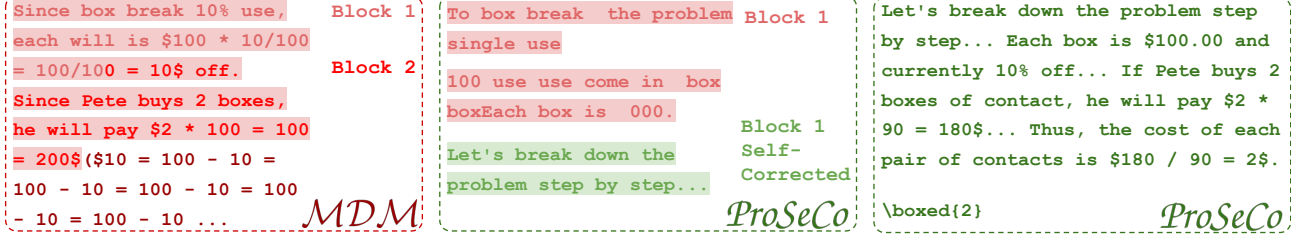


Figure 2. Demonstrating the benefits of self-correction (LLaDA baseline SFT vs. *ProSeCo* SFT; block AR decoding with 4 tokens generated at each step). (Left) During parallel unmasking errors occur. These mistakes accumulate, and by the 3rd block of generated text, the sample has collapsed. (Middle) *ProSeCo* can self-correct and recover from errors. After the first block, a short correction loop steers generation ‘back on track.’ (Right) *ProSeCo*’s ability to directly alter previously decoded tokens leads to a final high quality output. (Generated sequences are trimmed for illustrative purposes; see Appendix C.1 for full details).

where  $\dot{\alpha}_t$  denotes the time derivative of the noise schedule,  $\delta_{\mathbf{a}, \mathbf{b}} := \delta(\mathbf{a}, \mathbf{b})$  is the Kronecker delta function that evaluates to 1 if  $\mathbf{a} = \mathbf{b}$ ,  $\mathbb{E}_{q_{\text{data}}}$  refers to the expectation over drawing data samples  $\mathbf{x}^{1:L} \sim q_{\text{data}}$ , and  $\mathbb{E}_{q_t}$  is the expectation over drawing noisy latents from the forward marginals  $\mathbf{z}_t^{1:L} \sim q(\mathbf{z}_t^{1:L} \mid \mathbf{x}^{1:L})$ . We optimize this objective via stochastic gradient descent using Monte Carlo samples for the expectations and  $t \sim \mathcal{U}[0, 1]$  to approximate the integral.

A key drawback of this paradigm is that the denoising network  $\mathbf{x}_\theta$  does not learn to modify unmasked inputs  $\mathbf{z}_t \neq \mathbf{m}$ . Without the ability to correct mistakes, during generation, errors propagate and accumulate over time, causing the sampling trajectory to deviate from the true data distribution.

### 3. Self-Correcting Masked Diffusion Models

In this work, we aim to equip MDMs with the ability to alter previously decoded tokens. Our approach is to have a single model that can act in two ‘modes’: when inputs contain masked tokens, the model’s role is to unmask; when inputs contain all non-mask tokens, the model operates in ‘corrector’ mode and can update already generated positions.

Below, we present an augmented objective that trains models to jointly unmask and correct mistaken unmasked tokens. Our key insight is that during generation,  $\mathbf{x}_\theta$  produces unmasked tokens at each position, some of which align with the true data distribution and some of which potentially contain errors or distributional misalignment. A subset of these tokens are then carried into the next round of iterative refinement. We can interpret the outputs of  $\mathbf{x}_\theta$  as corrupted sequences from the data distribution, where certain tokens have been replaced by incorrect ones sampled from  $\mathbf{x}_\theta$ . This perspective motivates our formulation of model-generated sequences serving as inputs for a corrector model.

In Section 3.1, we introduce a straightforward corrector loss that we add to the MDM objective from (3), and in Section 3.2, we detail an easy to implement training algorithm to efficiently and jointly train a model to unmask and

correct decoding errors. Finally, in Section 4, we provide a sampling algorithm that leverages these abilities to further improve sample quality by interleaving error correction predictions and unmasking steps. Owing to this enhanced ability to iteratively refine any part of the sequence, including already decoded tokens, we dub our method *Progressive Self-Correction* (*ProSeCo*).

#### 3.1. Self-Correcting Objective

The high level idea of our approach is to train a corrector model to minimize the error between outputs from the denoiser and clean data. By tying weights of the corrector and denoiser networks, we turn this formulation into an augmented MDM variational objective with an auxiliary error correction loss.

More precisely, let  $\pi : \Delta^V \rightarrow \mathcal{V}$  be a transformation that generates samples from the MDM denoiser model. Then we define the input to our corrector as  $\mathbf{y}_t^{1:L} := (\pi \circ \mathbf{x}_\theta^1(\mathbf{z}_t^{1:L}), \dots, \pi \circ \mathbf{x}_\theta^L(\mathbf{z}_t^{1:L}))$ . For example,  $\pi$  could be the argmax function which returns the one-hot vector corresponding to the most likely sample at each position.

We present the following objective for training a corrector model alongside the standard MDM denoiser:

$$\mathcal{L}^{\text{CMDM}}(\phi, \theta) := \mathbb{E}_{q_{\text{data}}} \int_0^1 \mathbb{E}_{q_t} \sum_{\ell=1}^L \left[ \underbrace{\lambda \log \langle \mathbf{x}_\phi^\ell(\mathbf{y}_t^{1:L}), \mathbf{x}^\ell \rangle}_{\mathcal{L}^C} + \underbrace{\frac{\dot{\alpha}_t}{1 - \dot{\alpha}_t} \delta_{\mathbf{z}_t^\ell, \mathbf{m}} \log \langle \mathbf{x}_\theta^\ell(\mathbf{z}_t^{1:L}), \mathbf{x}^\ell \rangle}_{\mathcal{L}^{\text{MDM}}} dt \right], \quad (4)$$

where  $\phi$  denote the parameters of a corrector model  $\mathbf{x}_\phi^\ell(\mathbf{y}_t^{1:L}) \in \Delta^V$ . The standard MDM loss in the second term ensures that we train a useful denoiser  $\mathbf{x}_\theta$  that generates meaningful candidates for  $\mathbf{x}_\phi$  to correct. In addition to the MDM objective, we add a correction loss  $\mathcal{L}^C$  to every term in the integrand. This auxiliary loss amounts to a simple cross-entropy (CE) term, which encourages the model to identify and correct mistakes from the original denoising

network. The hyperparameter  $\lambda < 0$  lets us control the relative weight between the correction and diffusion losses.

We now detail design decisions that we found to be performant when using this modified objective.

**Tying Corrector and Denoiser Weights** In order to have a unified model that can both decode and correct, we elect to tie the weights  $\phi = \theta$ . This decision has the added benefit of eliminating memory overhead for training a separate corrector model. The error correction term in (4) thus becomes a self-correcting one:  $\mathcal{L}^C \rightarrow \mathcal{L}^{SC}$

**Selecting the Transformation  $\pi$**  To simplify optimization and ensure a deterministic mapping from  $\mathbf{z}_t^{1:L}$  to  $\mathbf{y}_t^{1:L}$  we use  $\arg \max$  sampling from  $\mathbf{x}_\theta(\mathbf{z}_t^{1:L})$ . This decision also aligns with how state-of-the-art MDMs, such as LLaDA (Nie et al., 2025), are used in practice. Namely, during generation, at every iteration, each masked position from the output of  $\mathbf{x}_\theta$  is decoded greedily. Then using some algorithm or heuristic, we determine which positions to retain for the next round and which to keep masked.

**Setting Corrector Loss Weight  $\lambda$**  We found empirically that a performant strategy was to set  $\lambda = \dot{\alpha}_t / (1 - \alpha_t)$ , that is, we reuse the same factor from MDM. In addition to balancing both terms in our objective, this weighting scheme is justified intuitively. Specifically, in the MDM objective the weight  $\dot{\alpha}_t / (1 - \alpha_t)$  will discount samples that are more heavily noised. For example, for the commonly used linear noise schedule  $\alpha(t) = 1 - t$ , this term amounts to dividing by the expected proportion of masked tokens in a sequence, i.e., we discount the ‘harder’, more heavily masked sequences. For training the corrector model, it is reasonable to apply a similar rationale: sequences with heavy masking which are harder to denoise will also be harder to correct and should therefore be down-weighted.

Combining the above, yields our objective for effective joint training of a unified denoising and self-correcting model:

$$\mathcal{L}^{SCMDM}(\theta) := \mathbb{E}_{q_{\text{data}}} \int_0^1 \mathbb{E}_{q_t} \frac{\dot{\alpha}_t}{1 - \alpha_t} \sum_{\ell=1}^L \left[ \underbrace{\log \langle \mathbf{x}_\theta^\ell(\mathbf{y}_t^{1:L}), \mathbf{x}^\ell \rangle}_{\mathcal{L}^{SC}} + \underbrace{\delta_{\mathbf{z}_t^\ell, \mathbf{m}} \log \langle \mathbf{x}_\theta^\ell(\mathbf{z}_t^{1:L}), \mathbf{x}^\ell \rangle}_{\mathcal{L}^{MDM}} dt \right], \quad (5)$$

### 3.2. Training with the $SCMDM$ Objective

In Algorithm 1, we present training for *ProSeCo*, which requires only minor modification to the standard MDM training in order to implement the new  $\mathcal{L}^{SCMDM}$  objective. Specifically, in addition to the standard MDM forward pass used for (3), we sample from  $\mathbf{x}_\theta$ , perform a second forward

pass, and incorporate the corrector loss. A final modification that we make to (5) is to wrap the denoiser model’s outputs in the stop-gradient operation  $\text{sg}(\cdot)$  prior to forming the corrector input, which ensures training stability.

#### Algorithm 1 *ProSeCo* Training

---

```

// Differences from standard MDM
// training highlighted in brown.
1: Input: Training data  $\mathcal{D}$ , model  $\mathbf{x}_\theta$  with parameters  $\theta$ , corruption process  $q$ , noise schedule  $\alpha_t$ .
2: repeat
3:   Sample  $\mathbf{x}^{1:L}$  i.i.d. from  $\mathcal{D}$ 
4:   Sample  $t \sim \mathcal{U}[0, 1]$ 
5:   Compute  $\alpha_t, \dot{\alpha}_t$ 
6:   Sample  $\mathbf{z}_t^{1:L} \sim q(\mathbf{z}_t^{1:L} \mid \mathbf{x})$ 
7:   Compute  $\mathbf{x}_\theta(\mathbf{z}_t^{1:L})$ 
8:    $\mathcal{L}^{MDM}(\theta) \leftarrow \frac{\dot{\alpha}_t}{1 - \alpha_t} \sum_{\ell=1}^L \delta_{\mathbf{z}_t^\ell, \mathbf{m}} \log \langle \mathbf{x}_\theta^\ell(\mathbf{z}_t^{1:L}), \mathbf{x}^\ell \rangle$ 
9:    $\mathbf{y}_t^\ell \leftarrow \text{sg}(\text{one\_hot}(\arg \max_i \mathbf{x}_\theta^\ell(\mathbf{z}_t)_i))$ , for  $\ell \in [1, L]$ 
10:  Compute  $\mathbf{x}_\theta(\mathbf{y}_t^{1:L})$ 
11:   $\mathcal{L}^{SC}(\theta) \leftarrow \frac{\dot{\alpha}_t}{1 - \alpha_t} \sum_{\ell=1}^L \log \langle \mathbf{x}_\theta^\ell(\mathbf{y}_t^{1:L}), \mathbf{x}^\ell \rangle$ 
12:  Perform gradient descent step on  $\mathcal{L}^{MDM}(\theta) + \mathcal{L}^{SC}(\theta)$ 
13: until converged
14: Return  $\theta$ 

```

---

## 4. Sampling with Progressive Self-Correction

In Algorithm 2, we present the sampling method for *ProSeCo*. Having a model that can jointly decode and correct allows us to interleave unmasking and correction steps. The goal of corrector iterations is two-fold: they should 1) potentially update already decoded positions in  $\mathbf{z}_t^{1:L}$  and 2) provide improved predictions to be used for sampling in the unmasking posterior. To control the computation budget allocated to self-correction, we allow users to specify hyperparameters that determines how often a self-correcting loop is executed,  $\omega$ , and the number of steps per loop,  $S$ .

In Algorithm 3, we present the procedure for applying self-correction. When entering this loop, we take  $\mathbf{x}_\theta(\mathbf{z}_t^{1:L})$  and convert it into a corrector input via  $\arg \max$  sampling at every position. Within each correcting iteration, we use a `sample` method, e.g., greedy-max decoding, to generate the next corrector input sequence from the corrector model outputs. After the inner loop completes, unmasked positions  $\mathbf{z}_t^\ell \neq \mathbf{m}$  are replaced with corresponding positions in the corrector sequence, which represents the remediation of already decoded tokens.

When operating as a strictly ‘unmasking’ model, an iteration of inference loop is identical to that in standard MDMs: the model’s input consists of a partially masked sequence  $\mathbf{z}_t^{1:L}$ , it outputs predictions  $\mathbf{x}_\theta^\ell(\mathbf{z}_t^{1:L})$  at every position  $\ell$ , and we decide some tokens to unmask via a call to a `sample_posterior` protocol, which returns a sequence with fewer masked tokens. For example, we can use `ances-`

**Algorithm 2** *ProSeCo* Sampling

---

```

// Differences from standard MDM
// sampling highlighted in brown.
1: Input: Model  $\mathbf{x}_\theta$ , length  $L$ , unmasking steps  $T$ , schedule  $\alpha_t$ ,
   self-correction budget (per step)  $S$ , corrector frequency  $\omega$ .
2: Initialize  $\mathbf{z}_{t(0)}^{1:L} \leftarrow \mathbf{m}^{1:L}$ 
3: for  $i = T$  to 1 do
4:   logits  $\leftarrow \mathbf{x}_\theta(\mathbf{z}_t^{1:L})$ 
5:   if  $(T - i + 1) \bmod \omega == 0$  then
6:      $\mathbf{z}_t^{1:L}$ , logits  $\leftarrow \text{corrector}(\mathbf{x}_\theta, S, \mathbf{z}_t^{1:L}, \text{logits})$ 
7:   end if
8:    $\mathbf{z}_{t(i-1)}^{1:L} \leftarrow \text{sample\_posterior}(\text{logits}, \mathbf{z}_t^{1:L}, \alpha_{t(i)})$ 
9: end for
10: Return  $\text{sample}(\mathbf{x}_\theta(\mathbf{z}_{t(0)}^{1:L}))$ 

```

---

tral sampling (Sahoo et al., 2024b), where we replace  $\mathbf{x}$  with  $\mathbf{x}_\theta$  in (2) and sample accordingly, the *confidence-based* approach proposed in Nie et al. (2025), where proposal tokens are selected greedily from  $\mathbf{x}_\theta(\mathbf{z}_t^{1:L})$  and those with top- $k$  confidence are retained for the next iteration, or one of other more recently proposed methods (Kim et al., 2025b;c; Ben-Hamu et al., 2025). If correction has been applied, instead of  $\mathbf{x}_\theta(\mathbf{z}_t^{1:L})$ , we use the corrector model’s last output for the `sample_posterior` routine, as the corrector model logits represent better informed predictions.

## 5. Experiments

### 5.1. Math & Code Benchmarks

**Setup** To evaluate *ProSeCo* on large MDMs, we perform supervised fine-tuning (SFT) of the LLaDA-Base 8B model (Nie et al., 2025) using our training Algorithm 1. Specifically, we SFT this model on the rStar-Coder (Liu et al., 2025) and OpenMathInstruct-2 (Toshniwal et al., 2024) datasets for  $\sim 40$  B tokens (see Appendix B.1 for full details). We then evaluate on downstream benchmarks for code: HumanEval (Chen et al., 2021) and MBPP (Austin et al., 2021b), and math: GSM8K (Cobbe et al., 2021) and Minerva (Hendrycks et al., 2021). In addition to reporting metrics for open-sourced large AR and MDM models (with and without corrector mechanisms), for a direct comparison to our approach, we apply our same SFT recipe using the standard MDM objective to LLaDA-Base.

Note that for all LLaDA-based models we apply the semi-AR sampling algorithm (Arriola et al., 2025) adopted by Nie et al. (2025), where the full generation sequence  $L$  is broken into blocks of size  $B$  and unmasking decoding is applied block-by-block from left-to-right (see Appendix A for an adaptation of Algorithm 2 to the block AR setting).

**Main Results** Table 1 represents our main results. The key finding is that for every benchmark, *ProSeCo* outperforms all diffusion baselines, including those coupled with other corrector mechanisms, and *ProSeCo* beats a comparably-sized

**Algorithm 3** *ProSeCo* Inner corrector loop

---

```

1: Input: Model  $\mathbf{x}_\theta$ , self-correction budget (per step)  $S$ , latent
   sequence  $\mathbf{z}_t^{1:L}$ , denoising output logits
2: Initialize  $\mathbf{y}_t^\ell \leftarrow \text{one\_hot}(\arg \max_i \text{logits}_i), \forall \ell \in [1, L]$ 
3: for  $S$  steps do
4:   corrector_logits  $\leftarrow \mathbf{x}_\theta(\mathbf{y}_t^{1:L})$ 
5:    $\mathbf{y}_t^{1:L} \leftarrow \text{sample}(\text{corrector\_logits})$ 
6: end for
   // Correct unmasked positions in  $\mathbf{z}_t^{1:L}$ 
7:  $\mathbf{z}_t^\ell \leftarrow \mathbf{y}_t^\ell, \forall \mathbf{z}_t^\ell \neq \mathbf{m}$ 
8: Return  $\mathbf{z}_t^{1:L}$ , corrector_logits

```

---

instruction fine-tuned AR model (Llama3.1; Grattafiori et al. (2024)) on three out of the four tasks. Moreover, we note that our baseline SFT model (fourth row from the bottom) represents a strong watermark, significantly improving over the LLaDA-Base and even surpassing / matching the LLaDA instruction fine-tuned model. Nevertheless, SFT using *ProSeCo* outperforms this strong baseline. Notably, even before applying the *ProSeCo* sampling procedure from Algorithm 2, the model trained with the *ProSeCo* objective outperforms one trained with the standard MDM loss.

**Analyzing the Quality-Efficiency Trade-off** In Figure 3, we present an analysis of the quality-efficiency trade-offs for *ProSeCo*. Results further to the north-west corner are desirable as they indicate better performance with a smaller number of function evaluations (NFEs).

In standard MDM, the only lever for controlling this trade-off is number of inference steps used for unmasking, or in other words the number of token positions generated in parallel at each decoding step. For *ProSeCo*, we can also control the compute via the frequency of corrector loops and number of iterative refinement steps per loop.

For each benchmark, we find that *ProSeCo* can outperform the highest accuracy baseline configuration, i.e., generating one token in each iteration; depicted as the gray dot. As depicted by the green star marker labeled as “Fast,” we can strictly improve baseline accuracy with reduced NFEs by increasing the decoding parallelism per unmasking step. To compensate for this, we apply corrector loops with some frequency (every 2-8 iterations, depending on the benchmark) and use up to 4 NFEs per corrector loop. Replacing unmasking steps with correcting ones, leads  $\sim 2\text{-}3$ x speed-ups relative to LLaDA decoding, while maintaining accuracy.

*ProSeCo* also enables configurations that can moderately increase compute while delivering significant accuracy improvements, as depicted by the orange star marker labeled as “Balanced” (for best trade-off; see Appendix B.1 for details on how this point was systematically selected). Finally, *ProSeCo* supports even further scaling of test-time compute to attain our highest performing results depicted in the blue star markers labeled as “Max.”

Table 1. Pass@1 accuracy on Code and Math benchmarks. ✗ / ✓ symbol in the ‘Corrector Sampling’ column indicates whether a correction sampling algorithm was applied. \* indicates values obtained via evaluation with open-sourced weights. † indicates values taken from Kim et al. (2025a). For models that we SFT, best value per column is **bolded** and second best is underlined.

		Corrector Sampling	Code		Math	
			HumanEval (0-shot)	MBPP (3-shot)	GSM8K (5-shot)	Minerva (4-shot)
<i>Off-the-Shelf 8B Models</i>						
<i>Baseline</i>	Llama3.1-Instruct* (Grattafiori et al., 2024)	✗	58.54	57.80	76.88	31.10
	LLaDA1.5* (Zhu et al., 2025)	✗	43.90	27.20	81.12	35.10
	LLaDA-Instruct* (Nie et al., 2025)	✗	40.24	29.40	78.85	33.32
	+ ReMDM* (Wang et al., 2025a)	✓	40.24	35.20	79.08	32.72
	+ PRISM† (Nie et al., 2025)	✓	42.70	32.30	—	—
<i>Our SFT with LLaDA-Base 8B Model</i>	LLaDA-Base* (Nie et al., 2025)	✗	33.54	40.40	66.72	27.88
	Vanilla SFT	✗	48.17	43.20	77.48	29.74
	+ ReMDM (Wang et al., 2025a)	✓	43.90	42.40	<u>80.97</u>	29.90
<i>Ours</i>	<i>ProSeCo</i> SFT	✗	<u>52.44</u>	<u>44.00</u>	79.45	<u>32.42</u>
	+ <i>ProSeCo</i> Sampling	✓	<b>62.20</b>	<b>50.20</b>	<b>82.18</b>	<b>35.10</b>

**Pareto Frontier for Parallel Decoding and Quality** Additionally, in Figure 4, we demonstrate that for standard MDMs, increasing the level of parallel decoding significantly degrades sample quality. In contrast, *ProSeCo* models can recover from the mistakes introduced during generation and better scale the parallel decoding-quality Pareto frontier.

**Ablation: Selecting Corrector Budget** Finally, in Appendix C.3 Figure 8, we explore the performance of various configurations of our sampling hyperparameters to provide guidance on allocating the corrector budget, as determined by frequency ( $\omega$ ) of and number of steps ( $S$ ) per loop. For fast sampling regimes (sampling steps  $\leq L/4$ ), where multiple tokens are decoded in parallel, we find that more frequent ( $\omega \geq$  sampling steps /16) corrector loops are required to overcome the drop in quality. In this regime, we also typically improve by performing more frequent and shorter corrector loops for a fixed number of maximum total corrector steps. For less parallel decoding (sampling steps  $\geq L/2$ ), *ProSeCo* outperforms the baseline with all the configurations we explored. Additionally, performance generally follows a monotonic upward trend as both frequency and number of corrector steps are increased.

## 5.2. Guided Molecule Design

In this context of guided generation, often when guidance strength is increased, model samples collapse. Our hypothesis is that *ProSeCo* can help recover from these errors, thereby improving the guided generation trade-off of maximizing some property of interest while still producing a diverse set of high quality samples.

**Setup** We follow the experimental setup from Schiff et al. (2024) (see Appendix B.2 for more details). Specifically, we

train models on string representations of molecules known as SMILES (Weininger, 1988) from the QM9 dataset (Rudigkeit et al., 2012; Ramakrishnan et al., 2014). We then apply the discrete classifier-free-guidance (CFG) algorithm from Schiff et al. (2024) with varying unmasking budgets  $T$  and guidance strength  $\gamma$ . We measure the number of generated sequences that are valid (can be parsed by RDKit library (Landrum et al., 2013)), unique, and novel (do not appear in the QM9 dataset) as the metric for diverse, high quality samples, and for the novel sequences, we compute the mean property value as the metric for property maximization. We perform this experiment for two properties: ring count and drug-likeness (QED; Bickerton et al. (2012)). We compare *ProSeCo* to an AR model, a diffusion model trained with uniform categorical noise (UDLM; Schiff et al. (2024)) a standard masked diffusion model (MDLM; Sahoo et al. (2024a)) and a remasking strategy applied to the MDLM model (ReMDM; Wang et al. (2025a)).

**Results** In Figure 5, we present the guidance results. Points further north-east are preferable, as they represent property maximization without sacrificing sample diversity and quality. For both properties of interest, *ProSeCo* pushes the Pareto frontier in the desired direction. This is particularly stark for experiments where we maximize the ring count property (left hand side of Figure 5).

## 5.3. Unconditional Text Generation

**Setup** Following Sahoo et al. (2024a), we train *ProSeCo* from scratch on the OpenWebText (OWT; Gokaslan & Cohen (2019)) dataset for 1M steps (see Appendix B.3 for full details). We then unconditionally generate 5000 samples consisting of  $L = 1024$  tokens, for varying sampling budgets  $T$ . We compute MAUVE (Pillutla

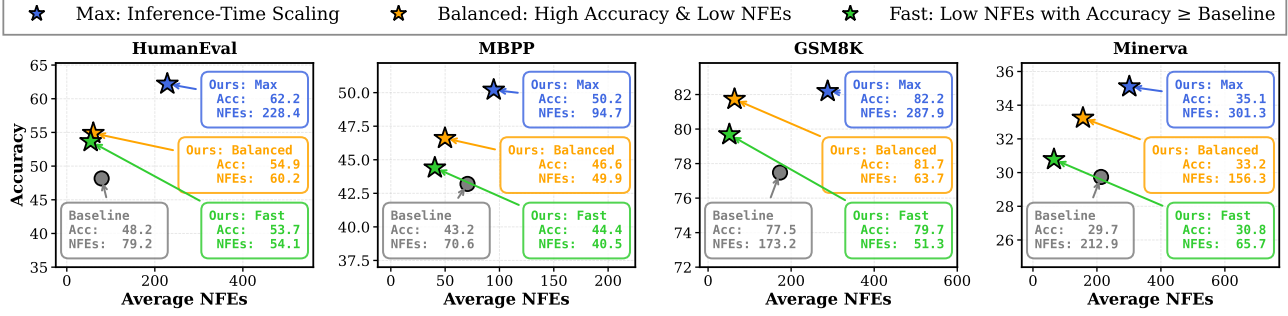


Figure 3. Analyzing the quality-efficiency trade-off for *ProSeCo*. Standard MDMs (Baseline; gray dot) attain best performance when decoding a single token in every step. *ProSeCo* models can vary number of corrector steps and attain comparable performance more efficiently with fewer unmasking steps (Ours: Fast; green star), achieve even better quality for modest increase in compute budget (Ours: Balanced; orange star), or maximize quality by scaling inference-time compute even further (Ours: Max; blue star).

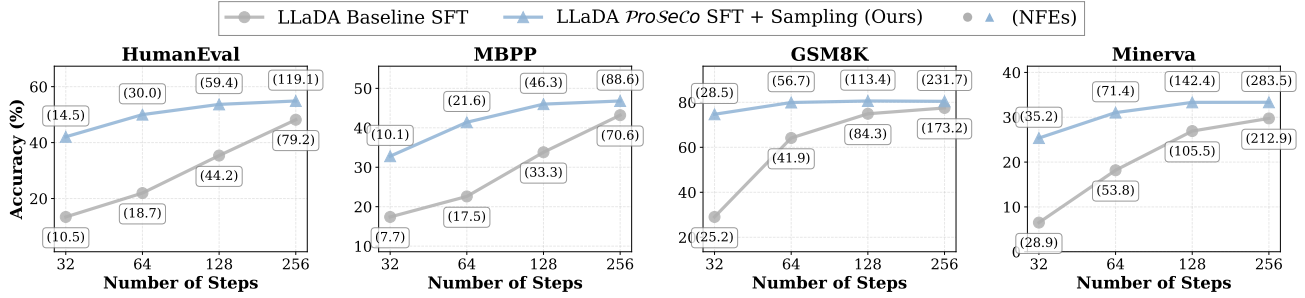


Figure 4. Pareto frontier of parallel decoding and quality. When decoding in parallel (i.e., fewer unmasking steps on  $x$ -axis), quality deteriorates. Applying a modest number of corrector steps, allows *ProSeCo* models to recover from these errors and extend this frontier.

et al., 2021) and report the perplexity under the GPT2-Large model (Radford et al., 2019), to also measure quality, and average sequence entropy, to reflect diversity of generated sequences (Zheng et al., 2024). We compare against an AR model and MDLM (Sahoo et al., 2024a) with and without corrector methods: ReMDM (Wang et al., 2025a) and PRISM (Kim et al., 2025a).

For *ProSeCo*, we apply a short, 3 step, corrector loop after each unmasking step. To maintain parity with the compute budget of the other methods, we reduce the number of unmasking steps by a factor of 4 per sampling budget  $T$ .

**Results** In Table 2, we see that across budgets, *ProSeCo* either significantly outperforms or matches baseline methods. Notably, even with just 256 steps, *ProSeCo* attains comparable sample quality to using PRISM with 2x or ReMDM with 4x the inference budget.

## 6. Related Works

**Discrete Diffusion** The seminal work of D3PM (Austin et al., 2021a) laid the foundation for adapting diffusion to discrete data. Some works extended this paradigm via the formalism of continuous-time Markov chains (Campbell et al., 2022; Lou et al., 2024). However, our method is more

in line with the continuous-time extensions of the variational inference perspective detailed in works, such as Ou et al. (2024); Sahoo et al. (2024b); Shi et al. (2024). Previous efforts in this vein have relied on categorical uniform noise corruptions (Schiff et al., 2024; von Rütte et al., 2025) to alleviate the locked-in decoded tokens limitation of MDMs. In contrast, our work maintains the original masking process and introduces a self-correcting loss term to enable updating of already decoded positions.

**Self-conditioning** Reusing a model’s prediction of the clean data via self-conditioning was found to be effective in Chen et al. (2022); Dieleman et al. (2022). However, in these works predictions are simply provided as an auxiliary input at each denoising step, whereas we use predictions to train self-correction and refine outputs during generation.

**Step Unrolling** Also related to our work is the concept of training on unrolled predictions from the denoising trajectory (Savinov et al., 2021). In this framework the model is trained on its own outputs of less noisy latent sequences, thereby more closely simulating the distribution seen during generation. Our method instead uses predictions of clean data, not unrolled trajectories of partially masked sequences.

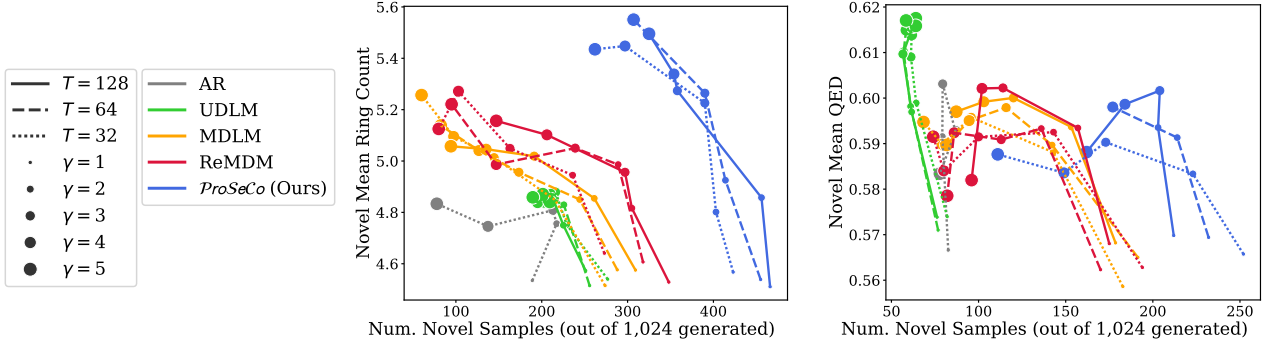


Figure 5. *ProSeCo* better navigates the novelty-property maximization Pareto frontier. Values correspond to number of novel samples (valid and unique molecules not present in the QM9 dataset;  $x$ -axis) and mean property value of novel samples ( $y$ -axis) for controlled generation using discrete classifier-free guidance (Schiff et al., 2024), with varying unmasking steps  $T$  (line style) and guidance strength  $\gamma$  (marker size). (Left) Maximizing the *ring count* property. (Right) Maximizing the *drug likeness (QED)* property.

Table 2. Unconditional generation sample quality for models trained on OpenWebText.  $\dagger$  Values reported in Kim et al. (2025a).  $\ddagger$  Values reported in Wang et al. (2025a).

Data	MAUVE ( $\uparrow$ )				Gen. PPL ( $\downarrow$ )				Entropy ( $\uparrow$ )			
	1.00				14.8				5.44			
AR ( $T = 1024$ ) $^{\ddagger}$	0.760				12.1				5.22			
$T =$	128	256	512	1024	128	256	512	1024	128	256	512	1024
MDLM $^{\dagger}$ (Sahoo et al., 2024a)	0.015	0.023	0.031	0.042	61.5	55.8	53.0	51.3	5.52	5.49	5.48	5.46
ReMDM $^{\dagger}$ (Wang et al., 2025a)	0.057	0.216	0.350	0.403	42.5	30.5	21.1	28.6	5.43	5.34	5.21	5.38
PRISM $^{\dagger}$ (Kim et al., 2025a)	0.118	0.294	0.423	<b>0.527</b>	21.5	18.0	16.4	15.3	5.18	5.15	5.12	5.10
<i>ProSeCo</i> (Ours)	<b>0.167</b>	<b>0.419</b>	<b>0.449</b>	0.523	19.7	14.9	12.5	11.1	5.26	5.19	5.12	5.06

**Corrector Methods** Several works have used a predictor-corrector framework to improve sample quality, where, following an unmasking predictor step, a corrector step is applied to remask decoded positions (Campbell et al., 2022; Gat et al., 2024; Peng et al., 2025; Wang et al., 2025a). In contrast to these training free methods, Lezama et al. (2023) and the concurrent works of Huang et al. (2025); Kim et al. (2025a); Liu et al. (2026) propose to train an additional head to predict incorrect positions that should be remasked.

More related to our work is Zhao et al. (2024b), which predicts corrections to already decoded tokens. However the method in Zhao et al. (2024a) relies on a distinct Hollow Transformer backbone (Sun et al., 2022). This severely limits its application to fine-tuning of MDMs pre-trained with the standard Transformer backbones, such as LLaDA.

## 7. Discussion & Conclusion

In this work, we presented a framework for jointly training a diffusion model to generate sequences via unmasking and self-correction. We enable and take advantage of this new ability via minimal and straightforward modifications to standard MDM training and sampling algorithms. Evaluating on conditional and unconditional generation, across various model sizes, we demonstrated that our method con-

sistently outperforms vanilla MDMs and alternative corrector methods both in terms of speed-quality tradeoffs and in the ability to further scale inference-time compute for improved generation.

**Limitations** The key drawback of our work is the added computational cost of the second forward pass during training, especially in contrast to inference-time only schemes, e.g., Wang et al. (2025a). However, the empirical results demonstrate that this trade-off of train-time compute is well worth the gains achieved on downstream evaluations.

**Future Directions** In follow up work, we plan to explore the disentangling of the corrector and unmasking models via weight untying or with completely separate neural network backbones for each model. Additionally, while we present a performant sampling algorithm, the ability to correct mistakes opens up the design space to more sophisticated schemes of jointly using corrector and unmasking steps, which we leave to future work to explore.

## Impact Statement

Our work falls within the domain of language modeling, and therefore, in addition to its potential benefits in accelerating

generation and improving quality, it is subject to related risks of misuse that are inherent with increasingly more powerful language modeling tools.

## Acknowledgments

This work was partially funded by the National Science Foundation under award CAREER 2145577, and by the National Institute of Health under award MIRA R35GM151243. Marianne Arriola is supported by a NSF Graduate Research Fellowship under award DGE-2139899 and a Hopper-Dean/Bowers CIS Deans Excellence Fellowship.

## References

Arriola, M., Gokaslan, A., Chiu, J. T., Yang, Z., Qi, Z., Han, J., Sahoo, S. S., and Kuleshov, V. Block diffusion: Interpolating between autoregressive and diffusion language models. *arXiv preprint arXiv:2503.09573*, 2025.

Austin, J., Johnson, D. D., Ho, J., Tarlow, D., and Van Den Berg, R. Structured denoising diffusion models in discrete state-spaces. *Advances in Neural Information Processing Systems*, 34:17981–17993, 2021a.

Austin, J., Odena, A., Nye, M., Bosma, M., Michalewski, H., Dohan, D., Jiang, E., Cai, C., Terry, M., Le, Q., et al. Program synthesis with large language models. *arXiv preprint arXiv:2108.07732*, 2021b.

Ben-Hamu, H., Gat, I., Severo, D., Nolte, N., and Kar rer, B. Accelerated sampling from masked diffusion models via entropy bounded unmasking. *arXiv preprint arXiv:2505.24857*, 2025.

Bickerton, G. R., Paolini, G. V., Besnard, J., Muresan, S., and Hopkins, A. L. Quantifying the chemical beauty of drugs. *Nature chemistry*, 4(2):90–98, 2012.

Bie, T., Cao, M., Chen, K., Du, L., Gong, M., Gong, Z., Gu, Y., Hu, J., Huang, Z., Lan, Z., et al. Llada2. 0: Scaling up diffusion language models to 100b. *arXiv preprint arXiv:2512.15745*, 2025.

Campbell, A., Benton, J., De Bortoli, V., Rainforth, T., Deli giannidis, G., and Doucet, A. A continuous time framework for discrete denoising models. *Advances in Neural Information Processing Systems*, 35:28266–28279, 2022.

Chen, M., Tworek, J., Jun, H., Yuan, Q., Pinto, H. P. D. O., Kaplan, J., Edwards, H., Burda, Y., Joseph, N., Brockman, G., et al. Evaluating large language models trained on code. *arXiv preprint arXiv:2107.03374*, 2021.

Chen, T., Zhang, R., and Hinton, G. Analog bits: Generating discrete data using diffusion models with self-conditioning. *arXiv preprint arXiv:2208.04202*, 2022.

Cobbe, K., Kosaraju, V., Bavarian, M., Chen, M., Jun, H., Kaiser, L., Plappert, M., Tworek, J., Hilton, J., Nakano, R., et al. Training verifiers to solve math word problems. *arXiv preprint arXiv:2110.14168*, 2021.

Dhariwal, P. and Nichol, A. Diffusion models beat gans on image synthesis. *Advances in neural information processing systems*, 34:8780–8794, 2021.

Dieleman, S., Sartran, L., Roshannai, A., Savinov, N., Ganin, Y., Richemond, P. H., Doucet, A., Strudel, R., Dyer, C., Durkan, C., et al. Continuous diffusion for categorical data. *arXiv preprint arXiv:2211.15089*, 2022.

Falcon, W. and The PyTorch Lightning team. PyTorch Lightning, March 2019. URL <https://github.com/Lightning-AI/lightning>.

Gao, L., Tow, J., Abbasi, B., Biderman, S., Black, S., DiPofi, A., Foster, C., Golding, L., Hsu, J., Le Noac'h, A., Li, H., McDonell, K., Muennighoff, N., Ociepa, C., Phang, J., Reynolds, L., Schoelkopf, H., Skowron, A., Sutawika, L., Tang, E., Thite, A., Wang, B., Wang, K., and Zou, A. A framework for few-shot language model evaluation, 12 2023. URL <https://zenodo.org/records/10256836>.

Gat, I., Remez, T., Shaul, N., Kreuk, F., Chen, R. T., Syn naeve, G., Adi, Y., and Lipman, Y. Discrete flow matching. *arXiv preprint arXiv:2407.15595*, 2024.

Gokaslan, A. and Cohen, V. Openwebtext corpus. <http://Skylion007.github.io/OpenWebTextCorpus>, 2019.

Grattafiori, A., Dubey, A., Jauhri, A., Pandey, A., Kadian, A., Al-Dahle, A., Letman, A., Mathur, A., Schelten, A., Vaughan, A., et al. The llama 3 herd of models. *arXiv preprint arXiv:2407.21783*, 2024.

Harris, C. R., Millman, K. J., van der Walt, S. J., Gommers, R., Virtanen, P., Cournapeau, D., Wieser, E., Taylor, J., Berg, S., Smith, N. J., Kern, R., Picus, M., Hoyer, S., van Kerkwijk, M. H., Brett, M., Haldane, A., del Río, J. F., Wiebe, M., Peterson, P., Gérard-Marchant, P., Sheppard, K., Reddy, T., Weckesser, W., Abbasi, H., Gohlke, C., and Oliphant, T. E. Array programming with NumPy. *Nature*, 585(7825):357–362, September 2020. doi: 10.1038/s41586-020-2649-2. URL <https://doi.org/10.1038/s41586-020-2649-2>.

Hendrycks, D., Burns, C., Kadavath, S., Arora, A., Basart, S., Tang, E., Song, D., and Steinhardt, J. Measuring mathematical problem solving with the math dataset. *arXiv preprint arXiv:2103.03874*, 2021.

Ho, J., Jain, A., and Abbeel, P. Denoising diffusion probabilistic models. *Advances in neural information processing systems*, 33:6840–6851, 2020.

Huang, Z., Wang, Y., Chen, Z., and Qi, G.-J. Don't settle too early: Self-reflective remasking for diffusion language models. *arXiv preprint arXiv:2509.23653*, 2025.

Hunter, J. D. Matplotlib: A 2d graphics environment. *Computing in Science & Engineering*, 9(3):90–95, 2007. doi: 10.1109/MCSE.2007.55.

Kim, J., Kim, S., Lee, T., Pan, D. Z., Kim, H., Kakade, S., and Chen, S. Fine-tuning masked diffusion for provable self-correction. *arXiv preprint arXiv:2510.01384*, 2025a.

Kim, J., Shah, K., Kontonis, V., Kakade, S., and Chen, S. Train for the worst, plan for the best: Understanding token ordering in masked diffusions. *arXiv preprint arXiv:2502.06768*, 2025b.

Kim, S. H., Hong, S., Jung, H., Park, Y., and Yun, S.-Y. Klass: Kl-guided fast inference in masked diffusion models. *arXiv preprint arXiv:2511.05664*, 2025c.

Kingma, D. P. Adam: A method for stochastic optimization. *arXiv preprint arXiv:1412.6980*, 2014.

Kingma, D. P. and Welling, M. Auto-encoding variational bayes. *arXiv preprint arXiv:1312.6114*, 2013.

Kuleshov, V. Fast algorithms for sparse principal component analysis based on rayleigh quotient iteration. In *International Conference on Machine Learning*, pp. 1418–1425. PMLR, 2013.

Landrum, G. et al. Rdkit: A software suite for cheminformatics, computational chemistry, and predictive modeling. *Greg Landrum*, 8(31.10):5281, 2013.

Lezama, J., Salimans, T., Jiang, L., Chang, H., Ho, J., and Essa, I. Discrete predictor-corrector diffusion models for image synthesis. In *The Eleventh International Conference on Learning Representations*, 2023.

Li, X., Thickstun, J., Gulrajani, I., Liang, P. S., and Hashimoto, T. B. Diffusion-lm improves controllable text generation. *Advances in Neural Information Processing Systems*, 35:4328–4343, 2022.

Liu, L., Huang, B., Liu, X., Yin, B., and Zhao, T. Teach diffusion language models to learn from their own mistakes. *arXiv preprint arXiv:2601.06428*, 2026.

Liu, Y., Zhang, L. L., Zhu, Y., Dong, B., Zhou, X., Shang, N., Yang, F., and Yang, M. rstar-coder: Scaling competitive code reasoning with a large-scale verified dataset. *arXiv preprint arXiv:2505.21297*, 2025.

Lou, A., Meng, C., and Ermon, S. Discrete diffusion modeling by estimating the ratios of the data distribution. In *Forty-first International Conference on Machine Learning*, 2024.

Nie, S., Zhu, F., You, Z., Zhang, X., Ou, J., Hu, J., Zhou, J., Lin, Y., Wen, J.-R., and Li, C. Large language diffusion models. *arXiv preprint arXiv:2502.09992*, 2025.

Ou, J., Nie, S., Xue, K., Zhu, F., Sun, J., Li, Z., and Li, C. Your absorbing discrete diffusion secretly models the conditional distributions of clean data. *arXiv preprint arXiv:2406.03736*, 2024.

pandas development team, T. pandas-dev/pandas: Pandas, February 2020. URL <https://doi.org/10.5281/zenodo.3509134>.

Paszke, A., Gross, S., Massa, F., Lerer, A., Bradbury, J., Chanan, G., Killeen, T., Lin, Z., Gimelshein, N., Antiga, L., Desmaison, A., Kopf, A., Yang, E., DeVito, Z., Raison, M., Tejani, A., Chilamkurthy, S., Steiner, B., Fang, L., Bai, J., and Chintala, S. PyTorch: An Imperative Style, High-Performance Deep Learning Library. In Wallach, H., Larochelle, H., Beygelzimer, A., d'Alché Buc, F., Fox, E., and Garnett, R. (eds.), *Advances in Neural Information Processing Systems 32*, pp. 8024–8035. Curran Associates, Inc., 2019.

Peebles, W. and Xie, S. Scalable diffusion models with transformers. In *Proceedings of the IEEE/CVF International Conference on Computer Vision*, pp. 4195–4205, 2023.

Peng, F. Z., Bezemek, Z., Patel, S., Rector-Brooks, J., Yao, S., Bose, A. J., Tong, A., and Chatterjee, P. Path planning for masked diffusion model sampling. *arXiv preprint arXiv:2502.03540*, 2025.

Pillutla, K., Swayamdipta, S., Zellers, R., Thickstun, J., Welleck, S., Choi, Y., and Harchaoui, Z. Mauve: Measuring the gap between neural text and human text using divergence frontiers. *Advances in Neural Information Processing Systems*, 34:4816–4828, 2021.

Radford, A., Wu, J., Child, R., Luan, D., Amodei, D., Sutskever, I., et al. Language models are unsupervised multitask learners. *OpenAI blog*, 1(8):9, 2019.

Ramakrishnan, R., Dral, P. O., Rupp, M., and Von Lilienfeld, O. A. Quantum chemistry structures and properties of 134 kilo molecules. *Scientific data*, 1(1):1–7, 2014.

Ruddigkeit, L., Van Deursen, R., Blum, L. C., and Reymond, J.-L. Enumeration of 166 billion organic small molecules in the chemical universe database gdb-17. *Journal of chemical information and modeling*, 52(11):2864–2875, 2012.

Sahoo, S. S., Arriola, M., Gokaslan, A., Marroquin, E. M., Rush, A. M., Schiff, Y., Chiu, J. T., and Kuleshov, V. Simple and effective masked diffusion language models. In *The Thirty-eighth Annual Conference on Neural*

Information Processing Systems, 2024a. URL <https://openreview.net/forum?id=L4uaAR4ArM>.

Sahoo, S. S., Gokaslan, A., Sa, C. D., and Kuleshov, V. Diffusion models with learned adaptive noise. In *The Thirty-eighth Annual Conference on Neural Information Processing Systems*, 2024b. URL <https://openreview.net/forum?id=loMa99A4p8>.

Savinov, N., Chung, J., Binkowski, M., Elsen, E., and Oord, A. v. d. Step-unrolled denoising autoencoders for text generation. *arXiv preprint arXiv:2112.06749*, 2021.

Schiff, Y., Sahoo, S. S., Phung, H., Wang, G., Boshar, S., Dalla-torre, H., de Almeida, B. P., Rush, A., Pierrot, T., and Kuleshov, V. Simple guidance mechanisms for discrete diffusion models. *arXiv preprint arXiv:2412.10193*, 2024.

Schwaller, P., Laino, T., Gaudin, T., Bolgar, P., Hunter, C. A., Bekas, C., and Lee, A. A. Molecular transformer: A model for uncertainty-calibrated chemical reaction prediction. *ACS central science*, 5(9):1572–1583, 2019.

Shi, J., Han, K., Wang, Z., Doucet, A., and Titsias, M. K. Simplified and generalized masked diffusion for discrete data. *arXiv preprint arXiv:2406.04329*, 2024.

Sohl-Dickstein, J., Weiss, E., Maheswaranathan, N., and Ganguli, S. Deep unsupervised learning using nonequilibrium thermodynamics. In *International conference on machine learning*, pp. 2256–2265. PMLR, 2015.

Song, Y. and Ermon, S. Generative modeling by estimating gradients of the data distribution. *Advances in neural information processing systems*, 32, 2019.

Song, Y., Sohl-Dickstein, J., Kingma, D. P., Kumar, A., Ermon, S., and Poole, B. Score-based generative modeling through stochastic differential equations. *arXiv preprint arXiv:2011.13456*, 2020.

Sun, H., Yu, L., Dai, B., Schuurmans, D., and Dai, H. Score-based continuous-time discrete diffusion models. *arXiv preprint arXiv:2211.16750*, 2022.

Toshniwal, S., Du, W., Moshkov, I., Kisacanin, B., Ayrapetyan, A., and Gitman, I. Openmathinstruct-2: Accelerating ai for math with massive open-source instruction data. *arXiv preprint arXiv:2410.01560*, 2024.

von Rütte, D., Fluri, J., Ding, Y., Orvieto, A., Schölkopf, B., and Hofmann, T. Generalized interpolating discrete diffusion. *arXiv preprint arXiv:2503.04482*, 2025.

Wang, G., Schiff, Y., Turok, G., and Kuleshov, V. d2: Improved techniques for training reasoning diffusion language models. *arXiv preprint arXiv:2509.21474*, 2025b.

Wang, Y., Schiff, Y., Gokaslan, A., Pan, W., Wang, F., De Sa, C., and Kuleshov, V. InfoDiffusion: Representation learning using information maximizing diffusion models. In Krause, A., Brunskill, E., Cho, K., Engelhardt, B., Sabato, S., and Scarlett, J. (eds.), *Proceedings of the 40th International Conference on Machine Learning*, volume 202 of *Proceedings of Machine Learning Research*, pp. 36336–36354. PMLR, 23–29 Jul 2023. URL <https://proceedings.mlr.press/v202/wang23ah.html>.

Waskom, M. L. seaborn: statistical data visualization. *Journal of Open Source Software*, 6(60):3021, 2021. doi: 10.21105/joss.03021. URL <https://doi.org/10.21105/joss.03021>.

Weininger, D. Smiles, a chemical language and information system. 1. introduction to methodology and encoding rules. *Journal of chemical information and computer sciences*, 28(1):31–36, 1988.

Wolf, T., Debut, L., Sanh, V., Chaumond, J., Delangue, C., Moi, A., Cistac, P., Rault, T., Louf, R., Funtowicz, M., et al. Huggingface’s transformers: State-of-the-art natural language processing. *arXiv preprint arXiv:1910.03771*, 2019.

Wu, C., Zhang, H., Xue, S., Liu, Z., Diao, S., Zhu, L., Luo, P., Han, S., and Xie, E. Fast-dllm: Training-free acceleration of diffusion llm by enabling kv cache and parallel decoding. *arXiv preprint arXiv:2505.22618*, 2025.

Yadan, O. Hydra - a framework for elegantly configuring complex applications. Github, 2019. URL <https://github.com/facebookresearch/hydra>.

Ye, J., Xie, Z., Zheng, L., Gao, J., Wu, Z., Jiang, X., Li, Z., and Kong, L. Dream 7b, 2025. URL <https://hkunlp.github.io/blog/2025/dream>.

Zhao, L., Ding, X., Yu, L., and Akoglu, L. Improving and unifying discrete&continuous-time discrete denoising diffusion. *arXiv preprint arXiv:2402.03701*, 2024a.

Zheng, K., Chen, Y., Mao, H., Liu, M.-Y., Zhu, J., and Zhang, Q. Masked diffusion models are secretly time-agnostic masked models and exploit inaccurate categorical sampling. *arXiv preprint arXiv:2409.02908*, 2024.

Zhu, F., Wang, R., Nie, S., Zhang, X., Wu, C., Hu, J., Zhou, J., Chen, J., Lin, Y., Wen, J.-R., et al. Llada 1.5: Variance-reduced preference optimization for large language diffusion models. *arXiv preprint arXiv:2505.19223*, 2025.

## A. Sampling with *ProSeCo* Semi-Autoregressively

In Algorithm 4, we present a modified version of our sampling method from Algorithm 2, which accommodates the block autoregressive decoding proposed in Arriola et al. (2025) and adopted by LLaDA (Nie et al., 2025). Given that we applied block AR decoding to the LLaDA models, the implementation provided in Algorithm 4 assumes full bidirectional attention is applied across the entire sequence at every forward pass, as in LLaDA, and is not written to support key-value (KV) caching. However, this algorithm can be adapted to support the efficient KV caching proposed in Arriola et al. (2025).

Notably, for *ProSeCo* with semi-AR decoding, at every correction iteration, clean tokens in the current block and all previously decoded blocks can be adapted.

---

### Algorithm 4 *ProSeCo* Sampling Block Autoregressive

---

```

// Assumes full bidirectional attention without KV-caching, as in LLaDA.
// Differences to standard MDM with block AR decoding highlighted in brown.
1: Input: Model  $\mathbf{x}_\theta$ , length  $L$ , block size  $B$ , unmasking steps  $T$ , noise schedule  $\alpha_t$ , self-correction budget (per step)  $S$ , corrector
   frequency  $\omega$ .
2: Initialize  $\mathbf{z}_{t(T)}^{1:L} \leftarrow \mathbf{m}^{1:L}$ 
3: for  $b = 1$  to  $(L/B)$  do
4:   for  $i = T$  to  $1$  do
5:     logits  $\leftarrow \mathbf{x}_\theta(\mathbf{z}_t^{1:L})$ 
6:     if  $(T - i + 1) \bmod \omega == 0$  then
7:        $\mathbf{z}_t^{1:L}$ , logits  $\leftarrow \text{corrector}(\mathbf{x}_\theta, \mathbf{z}_t^{1:L}, S)$ 
8:     end if
9:     logits $^\ell \leftarrow -\infty, \forall \ell \in [1, (b-1) \cdot B] \cup [b \cdot B + 1, L]$ 
10:     $\mathbf{z}_{t(i-1)}^{1:L} \leftarrow \text{sample\_posterior}(\text{logits}, \mathbf{z}_t^{1:L}, \alpha_{t(i)})$ 
11:   end for
12:    $\mathbf{z}_{t(0)}^{1:L} \leftarrow \text{sample}(\mathbf{x}_\theta(\mathbf{z}_{t(0)}^{1:L})), \forall \ell \in [1 + (b-1) \cdot B, b \cdot B]$ 
13:    $\mathbf{z}_{t(T)}^{1:L} \leftarrow \mathbf{z}_{t(0)}^{1:L}$ 
14: end for
15: Return  $\mathbf{z}_{t(0)}^{1:L}$ 

```

---

## B. Additional Experimental Details

### B.1. Math & Code Benchmarks

**Dataset** Our SFT dataset is a blend of the rStar-Coder (Liu et al., 2025) and OpenMathInstruct-2 (Toshniwal et al., 2024) datasets. Combined these datasets contain  $\sim 1.5$  M prompt-response pairs. Note that for the rStar-Coder, we remove reasoning traces from the dataset. We used the LLaDA-Instruct tokenizer and right-padded sequences up to a max length of 4096 tokens.

**Training Hyperparameters** We SFT the LLaDA-Base 8B model for  $\sim 40$  B tokens, which amounts to 6 epochs of training on our blended dataset. We train with a batch size of 512. For learning rate we linearly warm-up for 1000 gradient steps until a maximum learning rate of  $2e^{-5}$ . After this peak, we apply cosine decay until a minimum learning rate of  $2e^{-7}$ . We use the ADAM-w optimizer (Kingma, 2014) with beta parameters (0.9, 0.999). Finally, during training it is common to set a  $\text{min\_t} > 0$  value which biases the sampling of timesteps away from uniform over the unit interval, by shifting all samples to be in the range  $[\text{min\_t}, 1]$ . For example, in works such as Sahoo et al. (2024b), this value is set to  $1e^{-3}$ . For our SFT experiments, we found that biasing towards heavier masking during training led to improved performance, hence we set  $\text{min\_t}$  to  $1e^{-1}$ .

**Evaluation** For evaluation, we rely on the lm-eval harness library. We evaluate all models with batch size 1. This is to mitigate varying padding lengths based on prompt size variation and to enable effective use of early-stopping whenever the [EOS] token is generated.

We evaluate 4 benchmarks: HumanEval (Chen et al., 2021) and MBPP (Austin et al., 2021b), GSM8K (Cobbe et al., 2021) and Minerva (Hendrycks et al., 2021). For HumanEval we use 0-shot, for MBPP, we use 3-shot, for GSM8K 5-shot and for Minerva 4-shot, which corresponds to the defaults used for each of the benchmarks in their respective original proposals.

For LLaDA models, we use a semi-AR decoding scheme (Arriola et al., 2025), as in Nie et al. (2025), with default block

size of 32.

**Sampling Hyperparameters** When evaluating *ProSeCo* models, we explore different configurations of unmasking and corrector budgets. In Table 3, we detail the sampling hyperparameters used to generate the best performing results for *ProSeCo* reported in Table 1 and Figure 3; see Appendix C.2 for more details. Note that  $T$  represents a maximum unmasking budget, since we apply early stopping on the [EOS] token. Additionally,  $S$  represents a maximum corrector budget per correction loop, because we break the loop iterations if a corrector sequence does not change between rounds.

For Figure 4, we apply a corrector loop every 4 unmasking steps, with a maximum of 2 corrector iterations per loop.

Table 3. Sampling hyperparameters for results attained with *ProSeCo* and reported in Figure 3.

	HumanEval	MBPP	GSM8K	Minerva
<i>Maximum Accuracy</i>				
Accuracy (%)	62.20	50.20	82.18	35.10
Average NFEs	228.4	94.7	287.9	301.3
Maximum demasking steps $T$	256	128	128	128
Corrector frequency $\omega$	2	1	1	1
Maximum corrector steps per loop $S$	16	4	8	4
<i>Best Trade-off</i>				
Accuracy (%)	54.88	46.60	81.73	33.24
Average NFEs	60.2	49.9	63.7	156.3
Maximum demasking steps $T$	128	128	64	128
Corrector frequency $\omega$	4	4	4	4
Maximum corrector steps per loop $S$	4	4	4	4
<i>Fastest (Accuracy <math>\geq</math> Baseline)</i>				
Accuracy (%)	53.66	44.40	79.68	30.78
Average NFEs	54.1	40.5	51.3	65.7
Maximum demasking steps $T$	128	128	64	64
Corrector frequency $\omega$	8	8	8	8
Maximum corrector steps per loop $S$	4	4	4	4
<i>Baseline</i>				
Accuracy (%)	48.17	43.20	77.48	29.74
Average NFEs	79.2	70.6	173.2	212.9
Maximum demasking steps $T$	256	256	256	256

**Baselines** For all baseline results, other than PRISM (see below) we use open-source weights and evaluate using the lm-eval harness library, with batch size 1 and early stopping on the [EOS] token.

For ReMDM, we follow the algorithm proposed by Wang et al. (2025a) for applying this method to LLaDA. Namely, for each block of 32 tokens, once 28 tokens have been generated, we enable a ReMDM loop, where for 32 iterations we remask 2 tokens that had the lowest confidence at the time at which they were decoded and unmask 2 tokens based on their confidence. Hence, at the end of the ReMDM loop, there are still 28 unmasked and 4 masked tokens, at which point we finish generating using the standard LLaDA confidence-based sampling.

For PRISM (Kim et al., 2025a), since no open-source weights were available at the time of writing this manuscript, we use the values reported in their work. Note that the evaluation setup in PRISM is different than the one we use for the other entries in Table 1. Specifically, in PRISM the maximum generated sequence length is 1024, while we use sequence length 256. Additionally, for MBPP, PRISM reports 0-shot performance while we report 3-shot.

## B.2. Guided Molecule Design

For this experiment, we follow the setup detailed in Schiff et al. (2024).

**Dataset** We train on the QM9 dataset (Ruddigkeit et al., 2012; Ramakrishnan et al., 2014), which consists of  $\sim$ 133k molecules represented as SMILES strings (Weininger, 1988). We use the RDKit library (Landrum et al., 2013) to add the ring count and drug likeness (QED; Bickerton et al. (2012)) annotations. The dataset was tokenized using a regular expression tokenizer (Schwaller et al., 2019). We use sequence length of  $L = 32$ , with right-padding.

For each property, we generate binary labels that indicate whether a sample is below or above the 90th percentile of training samples. For discrete classifier-free-guidance (Schiff et al., 2024), we train with this label for conditional models, and randomly ‘drop it out’ 10 percent of the time by replacing it with a ‘masked’ label to simulate unconditional modeling.

**Hyperparameters** Hyperparameters follow Schiff et al. (2024). Namely, we use a DiT-style (Peebles & Xie, 2023) backbone with 92.4M parameters. Models were trained with a batch size 2048 and perform 25k gradient updates. We use a maximum learning rate of  $3e^{-4}$  that we linearly warm-up to for 1000 steps. After this peak we apply cosine decay until a minimum learning rate of  $3e^{-6}$ . We use the ADAM-W with beta parameters (0.9, 0.999).

Of note, when training *ProSeCo* models for ring count, we found it beneficial to eliminate the ‘copy over’ parameterization of the denoising network  $\mathbf{x}_\theta$  proposed in Sahoo et al. (2024a). That is, we do not enforce that  $\mathbf{x}_\theta$  simply copy over any token positions  $\mathbf{z}_t^\ell \neq \mathbf{m}$ . For training models, for the QED property, we maintained this copy-over parameterization.

**Evaluation** We generate 1024 samples from our model using various unmasking budgets  $T$  and guidance temperature  $\gamma$ . Of note, when applying the corrector model forward passes, we only use the conditional model, i.e.,  $\gamma = 1$ .

We use the RDKit library to parse generated samples. Of the valid strings (those that can be parsed) we retain unique samples that are not found in the original QM9 dataset (novel). We then use RDKit to measure the property of interest for these novel samples.

**Sampling Hyperparameters** For both ring count and QED maximization we use  $\omega = T/2$  for corrector loop frequency and  $S = T/16$  for steps per loop.

**Baselines** Values for the baseline models were taken from Wang et al. (2025a).

### B.3. Unconditional Text Generation

For this experiment we follow the setup described in Sahoo et al. (2024a).

**Dataset** We train models on the OpenWebText (OWT; Gokaslan & Cohen (2019)) dataset. We tokenized using the gpt-2 (Radford et al., 2019) tokenizer and created sequences of  $L = 1024$  tokens by wrapping samples and separating them with an [EOS] token. We also place an [EOS] token at the beginning and end of each sequence.

**Hyperparameters** As in Sahoo et al. (2024a), we use a DiT backbone with 170M parameters. We used a batch size of 512 and applied 1M gradient updates. We use a constant learning rate of  $3e^{-4}$  that we linearly warm-up to for 2500 steps. We use the ADAM-W optimizer with beta parameters (0.9, 0.999). As described in Appendix B.1, we use a `min_t` value of  $1e^{-1}$ , when training *ProSeCo* models on OWT.

**Evaluation** We follow the evaluation protocol from Wang et al. (2025a). Specifically, we generate 5000 samples and compute the MAUVE metric (Pillutla et al., 2021), generative perplexity under the gpt2-large model, and entropy of generated tokens.

**Sampling Hyperparameters** For *ProSeCo*, we match the inference budget of baseline results by using number of unmasking steps equal to  $T/4$  per column, performing a corrector loop at every iteration,  $\omega = 1$ , and applying 3 corrector steps per loop,  $S = 3$ .

**Baselines** Values for the baseline models were taken from Wang et al. (2025a), except for PRISM results which were taken from Kim et al. (2025a). For PRISM, results correspond to the ‘PRISM-loop’ method presented in Table 3 of Kim et al. (2025a).

## C. Additional Experimental Results

### C.1. Full Details for Figure 2

To generate the sequences presented in Figure 2, we took the prompt from the GSM8K test set corresponding to `doc_id: 584` in the lm-eval harness library. We generated a maximum sequence length of  $L = 512$  with blocks of size 32. We used

128 sampling steps, which translates to a parallel decoding factor of 4 tokens generated per step. For *ProSeCo*, we apply up to 8 corrector steps at the end of each block. In Table 6, we present the full prompt and generated sequences for the baseline and our models.

Figure 6. Example of *ProSeCo*'s self-correction enabling high quality generation, even with parallel decoding. Note, link breaks in the actual generated sequences were removed for clarity of presentation.

## C.2. Rules of Thumb for Correction Configurations

To characterize the quality-efficiency trade-offs of our model, we analyze the interaction between two primary hyperparameters: the *correction budget per step* ( $S \in \{1, 2, 4, 8, 16\}$ ) and the *correction frequency* ( $\omega \in \{1, 2, 4, 8\}$ ). We define the *correction intensity* as the ratio  $\rho = S/\omega$ . High values of  $\rho$  enable intensive iterative refinement between unmasking steps, while low values prioritize inference speed. A comprehensive analysis of this ratio is provided in Figure 7.

To navigate the Pareto frontier between quality and efficiency, we identify three configurations of practical interest, as visualized in our main results in Figure 3:

- **Max Accuracy Regime ( $\rho > 1$ ):** By allocating a larger budget to correction loops, the model prioritizes output quality and convergence. This regime explores the benefits of inference-time scaling, where additional computation is traded for higher accuracy. Our reported “Max Accuracy” points correspond to the configurations achieving the highest performance metrics within this group.
- **Fast Regime ( $\rho < 1$ ):** These configurations utilize sparse corrections relative to demasking. By interleaving minimal refinement steps, we effectively shift the Pareto frontier, achieving significant speedups with negligible accuracy degradation compared to the standard MDM baseline. We select these points by identifying the configuration with the lowest number of NFEs that maintains higher performance than the baseline.
- **Balanced Regime ( $\rho = 1$ ):** This serves as a controlled regime where correction steps are proportional to demasking steps. This regime ensures that total iterations do not exceed twice the number of demasking steps, providing a robust

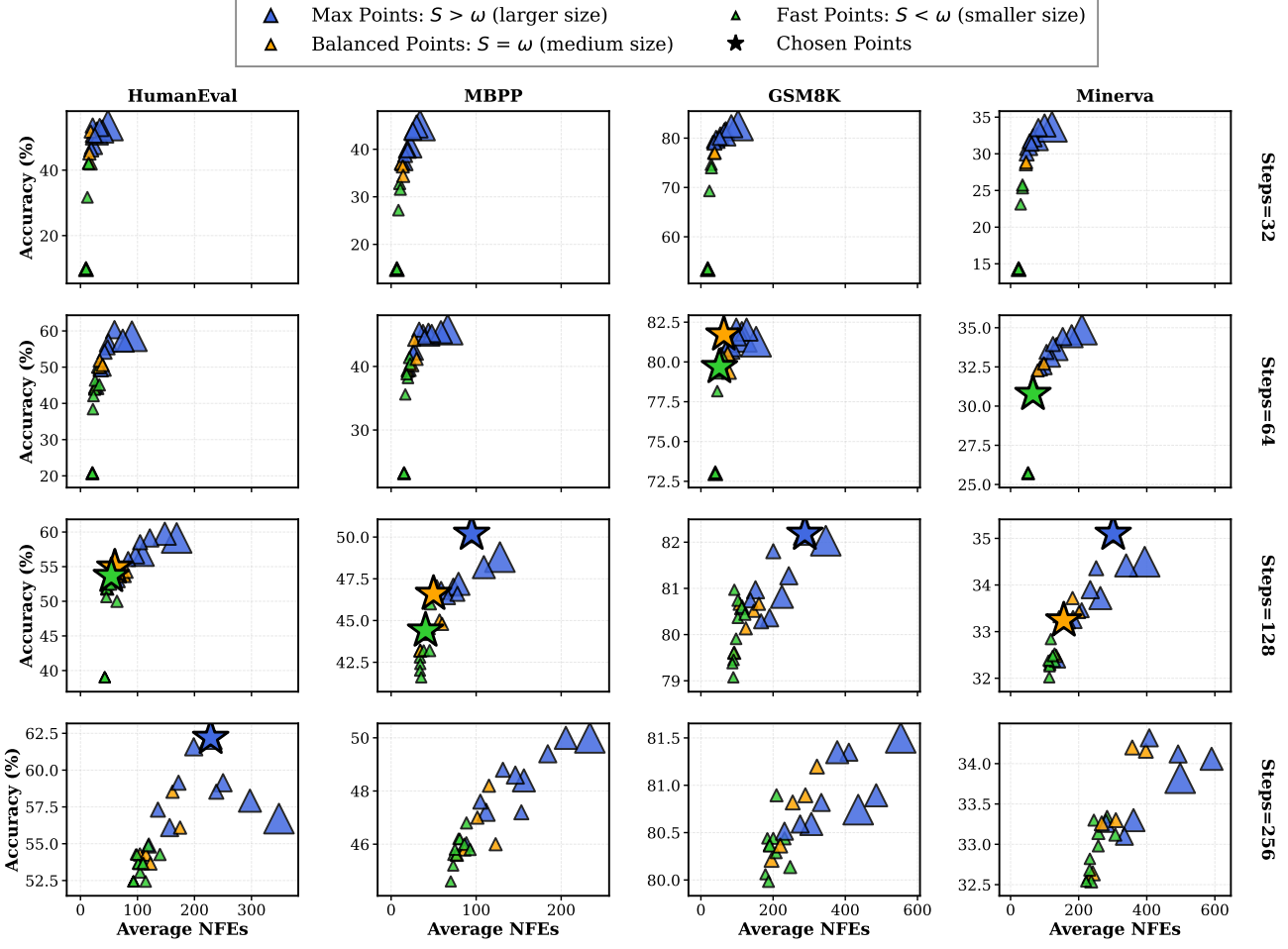


Figure 7. Illustration of the accuracy of *ProSeCo* across various benchmarks divided by groups: Max, Balanced and Fast points, defining by the correction intensity  $S/\omega$ . We evaluate our model by sweeping two primary parameters: the correction budget per step ( $S \in \{1, 2, 4, 8, 16\}$ ) and the correction frequency ( $\omega \in \{1, 2, 4, 8\}$ ). Markers size indicates the correction intensity value.

trade-off between latency and generative performance. We select these points by identifying the configuration closest to the normalized average of the Fast regime’s NFEs and the Max Accuracy regime’s performance.

### C.3. Ablation: Selecting Corrector Budget

In Figure 8, we provide results that help guide the selection of corrector budgets. In the first two rows, corresponding to ‘fast sampling’ regimes, we find that to overcome the degradation in sample quality from parallel decoding, we require correction frequency of at least  $\omega \geq T/16$ . Additionally, we see a general trend in this regime that, for a fixed corrector budget, more frequent but shorter correction loops are typically more effective.

When unmasking sampling steps increase ( $\geq L/2$ ), then we find the expected trend that scaling both frequency of correction loops and number of steps per loop leads almost uniformly leads to improved sample quality, at the cost of additional NFEs.

## D. Generated Samples

### D.1. LLaDA *ProSeCo* SFT Samples

In Figures 9 and 10, we present sample generations for the HumanEval and GSM8K datasets, respectively, using the maximum accuracy configuration for each benchmark (see Table 3).

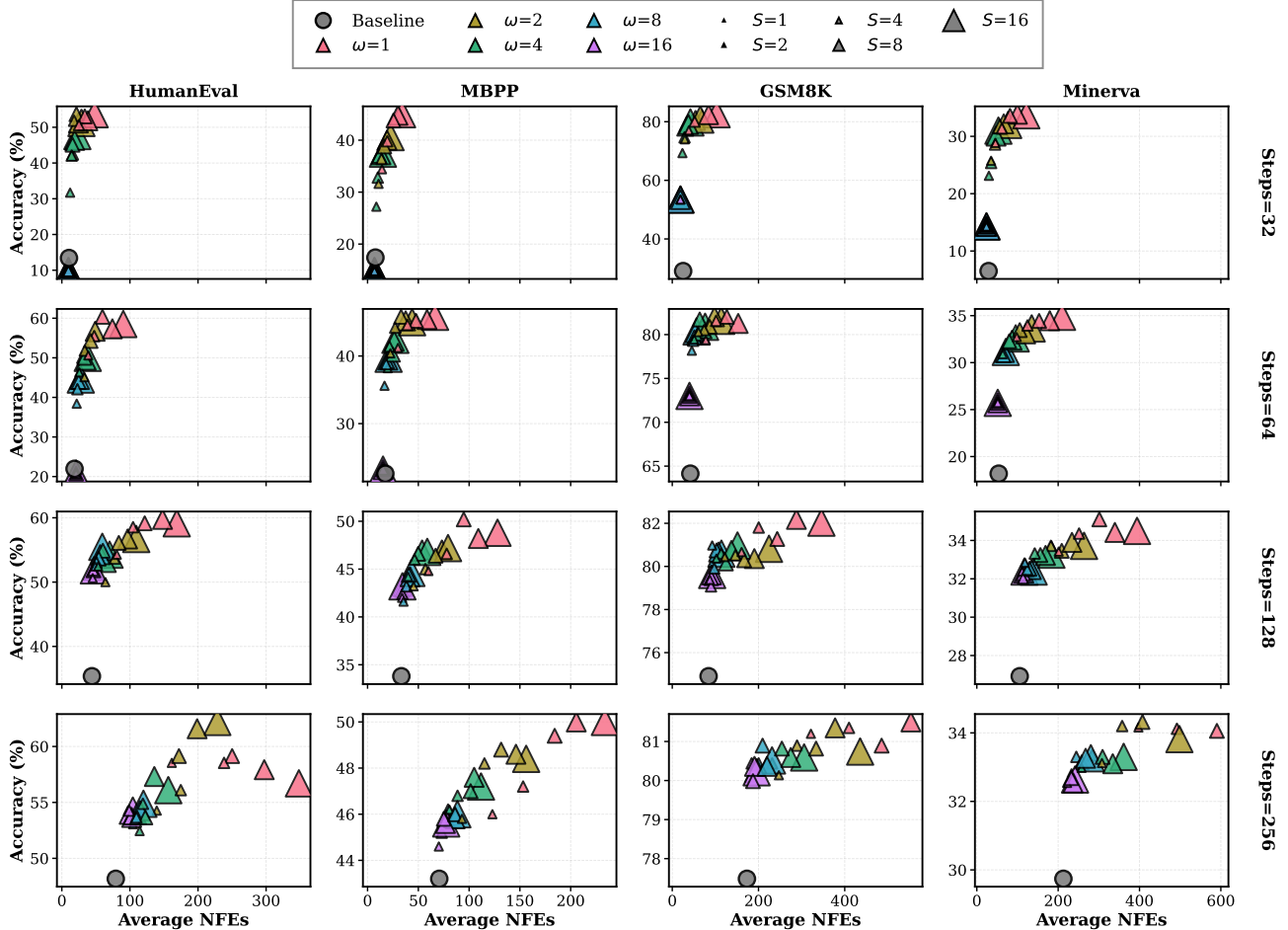


Figure 8. Ablation: Performance across various configurations of corrector steps. Frequency  $\omega \in \{1, 2, 4, 8, 16\}$  (denoted by color) and  $S \in \{1, 2, 4, 8, 16\}$  (denoted by marker size).

## D.2. *ProSeCo* Unconditional Generation Samples

In Figure 11, we present a sample generated from the *ProSeCo* model trained on OWT. We use total sample budget of  $T = 256$ , which consists of 64 unmasking steps, a corrector loop every  $\omega = 1$  step, and  $S = 3$  corrector steps per loop.

## E. Assets

In Table 4, we list the corresponding licenses for datasets used in this work.

Table 4. Datasets and corresponding licenses.

Dataset	License
GSM8K (Cobbe et al., 2021)	MIT
HumanEval (Chen et al., 2021)	MIT
MBPP (Austin et al., 2021b)	MIT
MinveraMath (Hendrycks et al., 2021)	MIT
OpenMathInstrcut-2 (Toshniwal et al., 2024)	CC BY 4.0
OpenWebText (Gokaslan & Cohen, 2019)	Creative Commons CC0 license (“no rights reserved”)
QM9 (Ruddigkeit et al., 2012; Ramakrishnan et al., 2014)	N/A
rStar-Coder (Liu et al., 2025)	CC BY 4.0

In Table 5, we list the corresponding licenses for software packages used in this work.

Table 5. Software and corresponding licenses.

Library	License
HuggingFace (Wolf et al., 2019)	Apache 2.0
Hydra (Yadan, 2019)	MIT
Fast-DLLM (Wu et al., 2025)	Apache 2.0
Language Model Evaluation Harness (Gao et al., 2023)	MIT
Matplotlib (Hunter, 2007)	Matplotlib license
Mauve (Pillutla et al., 2021)	GNU General Public License, Version 3
MDLM (Sahoo et al., 2024a)	Apache 2.0
NumPy (Harris et al., 2020)	NumPy license
OmegaConf	BSD 3-Clause
Pandas (pandas development team, 2020)	BSD 3-Clause “New” or “Revised”
PyTorch (Paszke et al., 2019)	BSD-3 Clause
PyTorch Lightning (Falcon & The PyTorch Lightning team, 2019)	Apache 2.0
RDKit (Landrum et al., 2013)	BSD 3-Clause “New” or “Revised”
Seaborn (Waskom, 2021)	BSD 3-Clause “New” or “Revised”
TorchMetrics	Apache 2.0
UDLM (Schiff et al., 2024)	Apache 2.0

**Prompt:**

```
from typing import List

def has_close_elements(numbers: List[float], threshold: float) -> bool:
    """ Check if in given list of numbers, are any two numbers closer to each other than given threshold.
    >>> has_close_elements([1.0, 2.0, 3.0], 0.5)
    False
    >>> has_close_elements([1.0, 2.8, 3.0, 4.0, 5.0, 2.0], 0.3)
    True
    """

```

**Answer:**

```
from typing import List

def has_close_elements(numbers: List[float], threshold: float) -> bool:
    numbers.sort()
    for i in range(len(numbers) - 1):
        if numbers[i+1] - numbers[i] < threshold:
            return True
    return False
```

**Prompt:**

```
def truncate_number(number: float) -> float:
    """ Given a positive floating point number, it can be decomposed into and integer part (largest integer smaller than given number) and decimals (leftover part always smaller than 1).
```

Return the decimal part of the number.  
 >>> truncate\_number(3.5)  
 0.5  
 """

**Answer:**

```
def truncate_number(number: float) -> float:
    return number - int(number)
```

Figure 9. Example of *ProSeCo*'s generated response on the HumanEval dataset using the max accuracy configuration (see Table 3).

**Prompt:**

Josh decides to try flipping a house. He buys a house for \$80,000 and then puts in \$50,000 in repairs. This increased the value of the house by 150%. How much profit did he make?

Let's break it down step by step:

1. Josh buys the house for \$80,000.
2. He puts in \$50,000 in repairs, so the total cost is \$80,000 + \$50,000 = \$130,000.
3. The value of the house increases by 150%, so the new value is \$80,000 \* 2.5 = \$200,000.
4. The profit is the difference between the new value and the total cost: \$200,000 - \$130,000 = \$70,000.

So, Josh made a profit of \boxed{70,000} dollars.

**Prompt:**

James decides to run 3 sprints 3 times a week. He runs 60 meters each sprint. How many total meters does he run a week?

Since James runs 3 sprints 3 times a week, he runs a total of  $3 \times 3 = 9$  sprints per week.

**Answer:**

Each sprint is 60 meters.

Thus, he runs a total of  $9 \times 60 = 540$  meters per week.

The answer is \boxed{540}.

Figure 10. Example of *ProSeCo*'s generated response on the GSM8K dataset using the max accuracy configuration (see Table 3).

|**endoftext**| you need to know where you're at if you want to make the exit.”

Between The Ghetto, In Theory, Ole T, and General Electric

In the fall of 2012, Andrew will open in Shazam, a venue that's underused for musical acts and comics, ranging from Pavement to Michael Jackson. When I sat him down for an interview, Andrew talked about reading Shazam "in ways people probably can't hear 'em, let alone sit down."

"Let's find out about our dreams," Andrew said. "Find out about our dreams and lives, where we came from and how we all grew up. It's crazy. I don't want to be a hippie, but I could be anything I want, and there's a lot of people in the world and everyone has their dreams. New York is where I grew up. I remember (2003) when there was the M.O.M.'s at the club, and I was one of the fans. It always had a mama-ish vibe. I call New York an awesome city. At first, I didn't know how many people there, but pretty soon you'd hear the same people all day.

"It's nice to get to sit in the humidor," I said, introducing him to the bouncer. "Honestly, now that you're at the club, it's really hard for people to relate to you (in New York). Because almost every guy will have something, but you only know the person personally, things that mean so much. It becomes something that stinks. But yeah, going to New York, being here, and being the bouncer and being [our] manager for another 10 years, you can always just move up here. You can live here, you can go to New York, and vice versa."

Andrew says he really still likes his New York feel. "It's not like I've moved up a lot, but it's still a city. A lot of people've grown up in this city," Andrew said. "I grew up in this neighborhood. When I was 10 years old, my friends went to this little dance club on Canal Street, and that's a little way off the block, but it's still a city.

"There are so many different people in New York City. Me and my friends grew up in the same neighborhood, but none of my friends moved here the same way. There are so many people who were in New York at the time but now they've gotten to New York, learning the language, learning the beat and rap and dance, you know, how to jump, how to do chords—everything. You get to go all the way up to New York. In fact, the only place that you know what the M.O.M. is—theapping, jumping, all the crazy stuff—is here."

When you head to New York City, it feels like a work in progress. In reality, for most people in New York, it's always been the same route: going to a dance club. Or, really, for some people at least, a dance club. And the M.O.C. is a dance club in New York.

"We're looking at it like, 'OK, aside from the idea, it's not happening right now. How do we fit in?'" Andrew said. "It's just different to us. We've been here for 10 years now, and people who went to the club 15 years back know how close it was to us. It was a whole different experience for us, and maybe we thought that it would be a bit different, but we were trying to figure it out and see how we fit in. I'm pretty sure that's exactly what happened."

"It's not what it is," Andrew said. "It's what I feel like in New York my whole life. I put on clothes for my underwear, and you know, shtography isn't that important, but just the clothes. A boxing ring. I go to the boxing gym every day, and I have two friends who know how to train too. We keep treating that time and trying to make sure we fit in, and it's gonna be that time."

Like many other people who say he's "strung in New York," Andrew said, "I definitely kind of feel grounded in New York."|**endoftext**|

Figure 11. Generated sample from *ProSeCo* trained on OWT, with a total budget of  $T = 256$ : 64 unmasking steps, corrector frequency  $\omega = 1$  and  $S = 3$  steps per loop.